Geophysical Research Letters

RESEARCH LETTER
10.1029/2024GL111080

Quantifying Salt Crystallization Impact on Evaporation Dynamics From Porous Surfaces

Sahar Jannesarahmadi[1], Milad Aminzadeh[1,2], Rainer Helmig[3], Dani Or[4,5], and Nima Shokri[1,2]

[1]Institute of Geo-Hydroinformatics, Hamburg University of Technology, Hamburg, Germany, [2]United Nations University Hub on Engineering to Face Climate Change at the Hamburg University of Technology, United Nations University Institute for Water, Environment and Health (UNU-INWEH), Hamburg, Germany, [3]Department of Hydromechanics and Modelling of Hydrosystems, University of Stuttgart, Stuttgart, Germany, [4]Department of Environmental Systems Science, ETH Zurich, Zurich, Switzerland, [5]Department of Civil and Environmental Engineering, University of Nevada, Reno, NV, USA

Key Points:

- Salt crystallization affected evaporative mass loss rates from sand samples
- Intermittent evaporation rate and surface temperature fluctuations were observed over sand surfaces
- Crystallization and dissolution processes changed the energy partitioning dynamics of evaporative sand samples

Supporting Information:

Supporting Information may be found in the online version of this article.

Correspondence to:

S. Jannesarahmadi, M. Aminzadeh and N. Shokri,
sahar.jannesarahmadi@tuhh.de;
milad.aminzadeh@tuhh.de;
nima.shokri@tuhh.de

Citation:

Jannesarahmadi, S., Aminzadeh, M., Helmig, R., Or, D., & Shokri, N. (2024). Quantifying salt crystallization impact on evaporation dynamics from porous surfaces. *Geophysical Research Letters*, *51*, e2024GL111080. https://doi.org/10.1029/2024GL111080

Received 2 JUL 2024
Accepted 30 OCT 2024

Author Contributions:

Conceptualization: Sahar Jannesarahmadi, Milad Aminzadeh, Rainer Helmig, Dani Or, Nima Shokri
Data curation: Sahar Jannesarahmadi
Formal analysis: Sahar Jannesarahmadi, Milad Aminzadeh
Funding acquisition: Nima Shokri
Investigation: Milad Aminzadeh, Dani Or, Nima Shokri
Methodology: Sahar Jannesarahmadi, Milad Aminzadeh, Nima Shokri
Supervision: Milad Aminzadeh, Nima Shokri
Writing – original draft: Sahar Jannesarahmadi

Abstract We investigated the effects of salt crystallization on the dynamics of saline water evaporation in porous media. Water mass loss rates from sand columns supplied with NaCl solutions at three concentrations were monitored under controlled ambient conditions. The formation and evolution of salt crystals over sand surfaces were synchronously imaged optically and thermally. Despite identical experimental and ambient conditions, we observed distinct crystallization dynamics that affected evaporative mass loss rates for similar salt concentrations, highlighting high variability of crystallization and its impact on evaporation. We observed the enhancement of maximum evaporation rates by factors of 3 to 14 under our experimental conditions and attributed this enhancement to the formation and evolution of porous crystalized salts at the surface. Additionally, visible intermittent temperature fluctuations of the salt crust were quantified using thermal imagery attributed to the dynamic processes of crystallization, dissolution and evaporation occurring simultaneously at the surface.

Plain Language Summary The impact of salt crystallization on the evaporation of saline water from porous media was experimentally investigated. We measured evaporative water loss rates from saturated sand columns and monitored the formation and evolution of salt crystals over the surface of samples through optical and thermal imaging. Notwithstanding identical experimental conditions, the formation of salt crystals affected the evaporation rates and surface temperature dynamics over samples with similar salt concentrations. Our findings provide insights into quantifying the impact of salt crystallization on altering mass loss dynamics from evaporating porous surfaces and associated changes in their surface energy balance.

1. Introduction

Evaporation of saline water from porous media influences several environmental and hydrologic processes ranging from soil salinization and crop production to ecosystem functioning, soil health and biodiversity (Dashtian et al., 2017; Hassani et al., 2020, 2024; Nachshon & Weisbrod, 2015). One of the mechanisms influencing soil salinization is soil water evaporation in the presence of soluble salt which affects salt concentration and distribution. During the evaporation process, the capillary-induced liquid flows transport the solute to the vapourization plane, while the diffusion process in the water phase tends to homogenize salt concentration throughout the porous medium. This competition is commonly quantified by the dimensionless Peclet number, Pe. When Pe number is larger than one, the solute is preferentially deposited close to the evaporation surface which could ultimately lead to salt crystallization and precipitation over the evaporating surface (Misyura, 2021; Shokri-Kuehni et al., 2022). Gradual increase in solution concentration near the evaporating surface may further induce density-driven flows, which are characterized by the Rayleigh number (D. A. Nield & Bejan, 2017; Wooding et al., 1997). In highly permeable porous media, these convective flows facilitate the downward transport of accumulated salt. On the other hand, instability flows are often impeded (or retarded) in low-permeability media, leading to the surface accumulation of salts and the formation of salt crystals (Bringedal et al., 2022). Salt crystallization is accompanied by dynamic energy exchange processes at the surface where exothermic crystallization reactions interplay with endothermic evaporative fluxes (Espinosa-Marzal & Scherer, 2010; Misyura, 2020; Shokri-Kuehni, Vetter, et al., 2017).

Writing – review & editing: Milad Aminzadeh, Rainer Helmig, Dani Or, Nima Shokri

Formation and evolution of crystalized salts are affected by various factors, including the type and concentration of salts, soil texture, grain angularity, moisture content, and atmospheric conditions (Dashtian et al., 2018; Derluyn et al., 2014; Jambhekar et al., 2016; Lasser et al., 2023; Lepinay et al., 2022; Licsandru et al., 2023; Nachshon, Weisbrod, et al., 2011; Norouzi Rad et al., 2015; Sghaier et al., 2014; Shokri-Kuehni, Norouzi Rad, et al., 2017; Shokri-Kuehni et al., 2018, 2022). Salt crystals nucleate in a finite number of nucleation sites often associated with fine pores filled with water at the evaporation surface (Norouzi Rad et al., 2013). Surface coverage by efflorescence salt crystals gradually increases as adjacent nuclei merge and form a salt crust over the surface (Nachshon et al., 2018).

Despite the impact of salt accumulation near the vapourization plane on reduction of saturated vapor pressure (Eloukabi et al., 2013), evaporative water loss may be enhanced (relative to freshwater evaporation from the same surface) by the capillary flow within the porous and wet efflorescence crust (Shahidzadeh-Bonn et al., 2008; Shokri-Kuehni et al., 2020). However, drying of the efflorescence eventually forms a diffusion barrier that may hinder evaporation rates (Nachshon, Shahraeeni, et al., 2011; Sghaier & Prat, 2009). In fine-textured porous media, formation of crusty efflorescence limits the evaporation by obstructing diffusive vapor fluxes. On the other hand, coarser media often exhibit patchy efflorescence patterns hydraulically connected to the surface that could enhance evaporative mass loss rates (Eloukabi et al., 2013). Spatial variation of evaporation flux affects development of the efflorescence where higher mass loss rate and greater transport length at the periphery of an evaporating surface increase the local Peclet number and lead to preferential growth of efflorescence (Eloukabi et al., 2013; Misyura, 2020). At the field scale, high evaporation rates lead to the surface accumulation of soluble salts and the formation of salt crusts in dry salt lakes or salt deserts (typically manifested as polygonal ridges) (Lasser et al., 2021). These salt crusts cover the lakebed or desert surface and, as they degrade, contribute to atmospheric dust emissions (J. M. Nield et al., 2015).

Despite advances in understanding evaporation of saline water from porous media, the presence of evolving porous salt crust on the surface and its coupling with flow characteristics within the underlying porous medium pose a challenge to quantitatively describe saline water evaporation and the subsequent adjustments to surface energy partitioning. The influence of crystallized salt on evaporative fluxes is not well understood, with several open questions remaining (see Shokri-Kuehni et al. (2022) for a detailed discussion). The present study thus aims at investigating the impact of porous crystallized salt on the dynamics of saline water evaporation from porous media. Specifically, we focus on the coupling between evaporation flux and surface temperature at the surface of salt crystals to understand how the crystallization process influences surface moisture distribution and local variations of surface temperature and evaporation.

2. Materials and Methods

We conducted a series of laboratory experiments under well-controlled ambient conditions to investigate the dynamics of salt crystallization (Figure 1). Glass cylindrical columns with diameter of 5 cm and height of 20 cm were filled with sand with particle sizes ranging from 0.4 to 0.8 mm, porosity of 0.38, and density of 2.65 g/cm^3 (see Jannesarahmadi et al. (2023) for details of water retention characteristics and pore size distribution). To quantify the contribution of drying-induced crystallization on evaporative fluxes, the sand columns were kept saturated during the evaporation process by maintaining a water table at the surface of samples using Marriott bottles. We conducted the experiments using brine with different NaCl concentrations of 10%, 15%, and 20% (mass basis). For repeatability of the results, we ensured that in each round of experiment, three sand columns were connected to Marriott bottles containing identical saline water concentration. Additionally, we used a fourth column supplied from a Marriott bottle with freshwater to serve as a reference for nonsaline evaporation rates.

The experiments were conducted in a climate chamber (Memmert, HPP750eco) with constant relative humidity of 30% and air temperature at 30°C. Water mass loss rates from the Marriott bottles were recorded every 10 min using digital balances (Kern EW 6200-2NM) with repeatability and linearity of 0.01 and 0.03 g, respectively. To delineate the formation and evolution of salt crystals during evaporation, the surface of the sand columns was synchronously monitored using a thermal imager (FLIR, A700 PROF) and an optical camera (Canon, EOS M50) at 10 min intervals. Infrared images with 640 × 480 pixels enabled capturing dynamics of surface temperature and thermal signatures associated with evaporation and crystallization processes at a spatial resolution of about 0.25 mm.

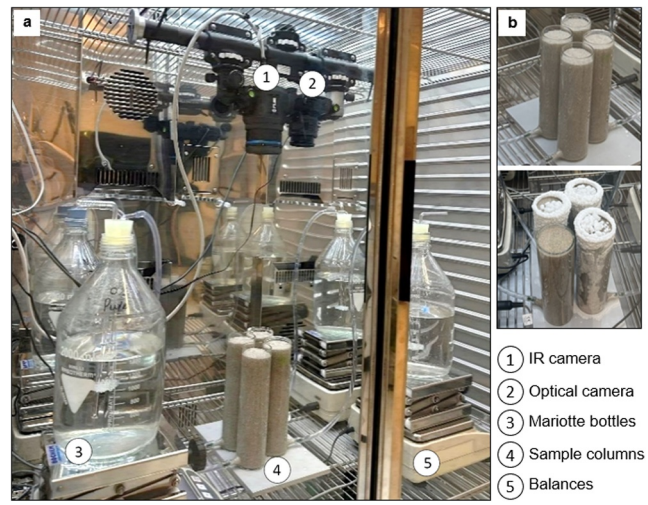

Figure 1. (a) The experimental setup in a climate chamber with controlled temperature and humidity. (b) Surface of columns at the beginning and at the end of the experiment.

3. Results and Discussion

Various aspects of the conducted experiments were investigated using the measured data by the balances and the cameras. In what follows, we present the results and describe their implications.

3.1. Cumulative Mass Loss and Evaporation Fluxes From Sand Columns

Figure 2a depicts the cumulative evaporative mass losses from sand samples at different concentrations of NaCl. Overall, increasing salt concentration leads to a more pronounced impact of crystallization on evaporation process, in agreement with the previous studies (Bringedal et al., 2022; Norouzi Rad et al., 2013). Despite maintaining identical experimental conditions, the sand samples with similar salt concentrations exhibited distinct evaporation dynamics possibly due to varying crystallization dynamics. This highlights the significant influence of porous salt crystals on the evaporation process (Dashtian et al., 2018; Shokri-Kuehni, Norouzi Rad, et al., 2017).

The fluxes of evaporation from the sand samples are shown in Figure 2b. As mentioned above, the samples remained saturated during the experiments by maintaining the water table at the surface of sand columns. Considering the controlled ambient conditions, the evaporation flux from the freshwater samples remained fairly constant, whereas gradual increase in ion concentrations near the vapourization plane primarily yielded a decreasing drying rate for the saline samples (Shokri-Kuehni et al., 2018). A significant decrease in the evaporation flux is observed for a sample of 10% (rep1) and a sample of 20% (rep3) NaCl concentration. This reduction can be attributed to the formation of a salt crust detached from the sand surface that hinders diffusive vapor fluxes into the air mass (Licsandru et al., 2022).

The disparity between the evaporation fluxes of fresh and saline water increased as salt crystals formed and grew over the surface. An intermittent pattern in the evaporation flux of saline samples was observed as the salt crystals were evolving. Our results highlight intensified fluctuations in evaporation fluxes with increase in salt concentration (Misyura, 2018). In addition, sand samples with identical salt concentration (in each round of experiment) demonstrated different fluctuation patterns. Hence, we used the gamma distribution to quantify differences in the observed intermittent evaporation fluxes since the onset of crystallization (Aminzadeh et al., 2017). Figure 2c displays the distribution function of the fluctuation times (τ_i) described by the gamma distribution. The mean fluctuation time ($\bar{\tau}$) is thus derived from the shape (α) and rate (β) parameters of the gamma function:

$$\phi(\tau) = \frac{\beta^{\alpha}}{\Gamma(\alpha)} \tau^{\alpha-1} e^{-\beta\tau} \tag{1a}$$

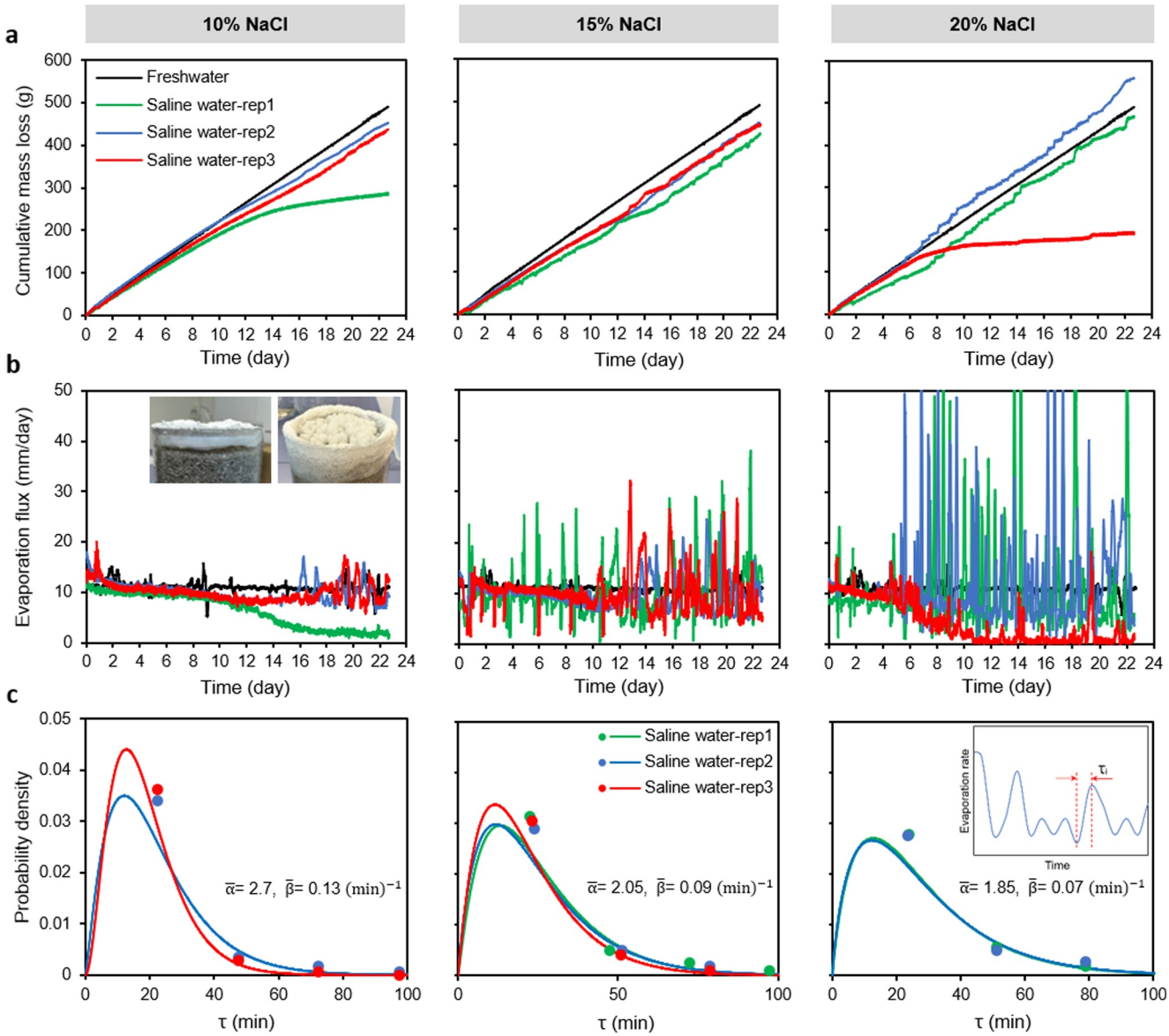

Figure 2. (a) Cumulative evaporative mass losses during evaporation from sand columns saturated with 10%, 15%, and 20% NaCl (mass basis). (b) Evaporation flux of samples with different salt concentrations. The inset compares the surface of a sample with detached salt crust (left) to a sample where the crust remains hydraulically connected to the surface (right). (c) Distribution functions of fluctuation times (symbols) described by the gamma distribution (curves). The inset shows the time between consecutive peaks and valleys in the evaporation flux signals. The evaporation fluxes of the samples with detached crust were excluded from the fluctuation analysis.

$$\bar{\tau} = \frac{\alpha}{\beta} \tag{1b}$$

Despite the visible variations in the fluctuation of the calculated evaporative fluxes in each round of the experiment, the distribution functions remained nearly identical among samples with similar concentrations. As the salt concentration increased, the broadness of the gamma function increased resulting in an increase in the mean fluctuation time ($\bar{\tau}$) from approximately 20 min in samples with 10% concentration to about 30 min in those with 20% concentration.

In the following section, we investigate thermal signatures at the surface of evaporating sand samples to provide insights into the effects of crystallization on the highly dynamic nature of mass loss rates from the saline samples relative to the freshwater sand column.

3.2. Thermal Signatures of Salt Crystallization

Formation and evolution of salt crystals on the surface of sand samples and their associated thermal signatures are illustrated in Figure 3a, indicating earlier crystallization for higher NaCl concentrations. In addition to different crystallization patterns over the surface of samples with different concentrations, IR thermography demonstrates complex temperature patterns of crystals as illustrated in the previous studies (Shokri-Kuehni, Vetter, et al., 2017; Shokri-Kuehni et al., 2020). The presence of cold spots indicates the contribution of wet crystallized salts in evaporation from the sample, which underscores the multifaceted role of crystallization dynamics in altering heat and mass transfer processes during evaporation. The solution is sucked up to the crystal surface where water evaporates and leads to salt precipitation and crystal growth at the air-solution interface (Lazhar et al., 2020; Rodriguez-Navarro & Doehne, 1999; Shokri-Kuehni, Norouzi Rad, et al., 2017). The complex interplay between latent heat cooling, exothermic salt precipitation, and endothermic dissolution processes causes surface temperature fluctuations. Formation and dissolution of salt crystals change surface temperature, resulting in the appearance and disappearance of temperature spikes in IR images.

We employed the surface energy balance equation to provide a quantitative estimate of the heat fluxes arising from crystallization (or dissolution) process over the surface of evaporating sand samples:

$$q_{\text{rad}} - q_{\text{evap}} + q_{\text{conv}} + q_{\text{cond}} + q_{\text{cr}} = 0 \tag{2}$$

where q_{rad} is radiation flux (W/m^2), q_{evap} is evaporation flux (W/m^2), q_{conv} is convection heat exchanges with overlying air (W/m^2), q_{cond} is conduction heat flux with sand column beneath (W/m^2), and q_{cr} accounts for the average heat flux released during crystallization process (W/m^2) (negative sign stands for the assumed outgoing heat fluxes). All fluxes have been represented per flat surface of the sand columns (A_f). In the absence of shortwave radiation flux in our experiments, q_{rad} only represents the longwave exchanges between the surface and the surrounding ambient. The average flux of crystallization over the evaporating surface could thus be estimated by rearrangement of Equation 2:

$$q_{\text{cr}} = -\frac{A_s}{A_f}\left(\sigma\varepsilon_a T_a^4 - \sigma\varepsilon_s T_s^4\right) + q_{\text{evap}} - \frac{A_s\, k_a}{A_f\, \delta}(T_a - T_s) - \frac{k_{\text{soil}}}{Z}(T_Z - T_s) \tag{3}$$

in which ε_s and ε_a are surface and ambient emissivity, respectively, σ is the Stefan-Boltzmann constant (5.67×10^{-8} W/m^2 K^4), k_a and k_{soil} are thermal conductivity of air and soil (W/mK), respectively, δ is the thickness of air boundary layer (m) (estimated based on water mass loss rates from freshwater sample), T_s is surface temperature, T_a is ambient air temperature, and T_Z (K) is soil temperature at thermal decay depth Z (m) below the surface (Shahraeeni & Or, 2010). See Section 3.3 for details of estimating the ratio of increased surface area of evaporating samples due to formation of salt crusts relative to the flat plate area (A_s/A_f).

Figure 3b depicts variations of q_{cr} for samples with different salt concentrations. Negative values of q_{cr} refers to the absorbed heat during dissolution of salts over the surface. These results indicate that formation and dissolution of salt crystals lead to alternation of surface energy balance with associated variations of surface temperature (see details in Figure S1 and Table S1 of Supporting Information S1). The exothermic nature of the crystallization yields increases in the surface temperature with formation and growth of salt crystals (Shokri-Kuehni, Norouzi Rad, et al., 2017). The enthalpy of crystallization (38.9 kJ/kg) and associated heat released at the surface may explain the abrupt increases in evaporation rates from sand samples (Derluyn, 2012). On the other hand, the endothermic dissolution of salt crystals yields temperature drop at the surface that is accompanied by reduction of evaporative loss due to the temperature dependence of saturated vapor concentration (Aminzadeh et al., 2016; Aminzadeh & Or, 2013; Misyura, 2018, 2020). As shown in Figure 3c, crystallization events are accompanied by dissolution processes. Growing crystals consume the supersaturated solution, potentially leading to the dissolution of nearby crystals. Additionally, the increase in surface temperature with crystal formation raises the solubility of the solution, further facilitating dissolution of existing crystals. Similar fluctuations in surface

10.1029/2024GL111080

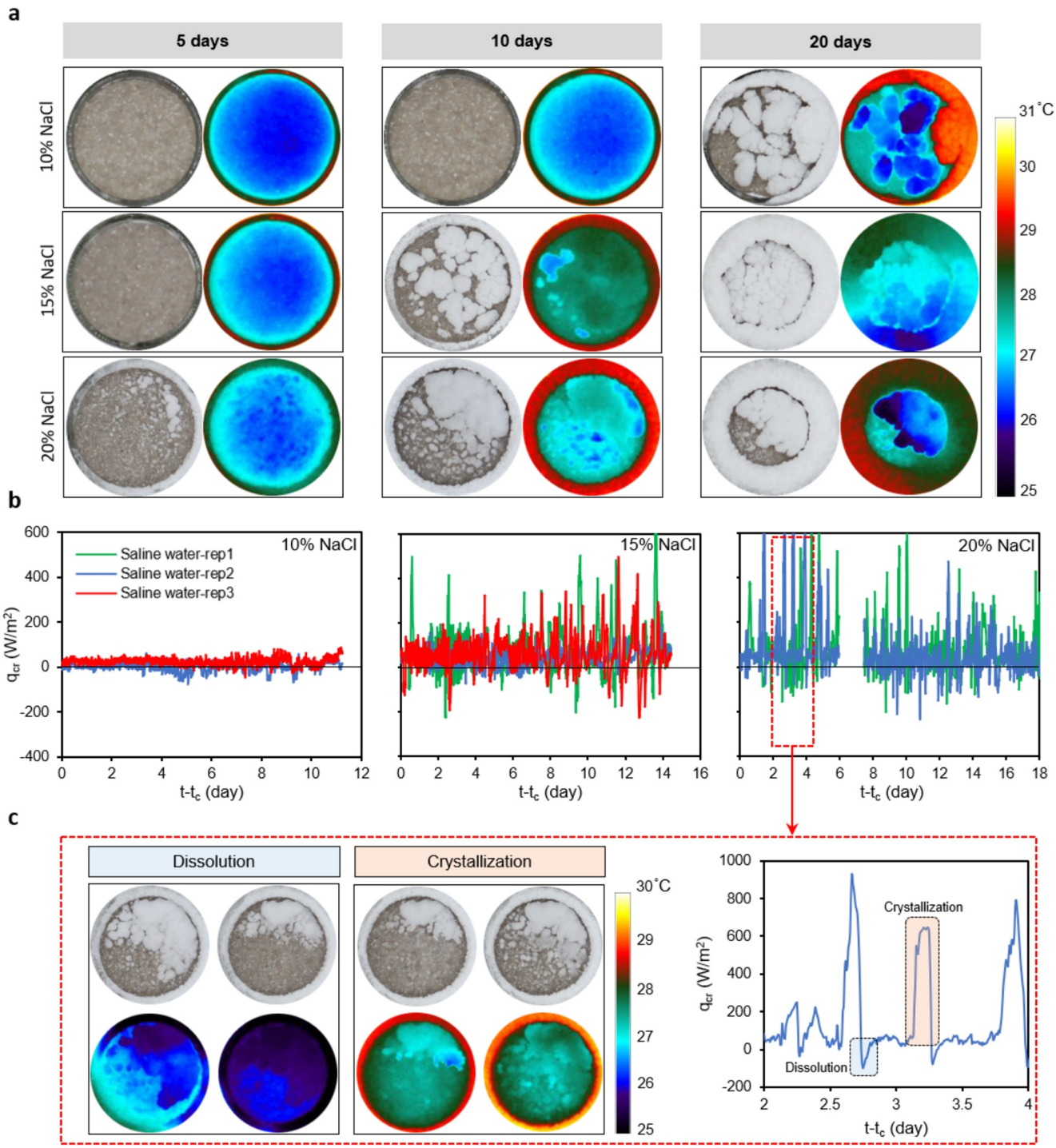

Figure 3. (a) Precipitation patterns and thermal signatures captured by optical and thermal cameras at different days for samples saturated with 10%, 15%, and 20% NaCl solutions. The colorbar indicates the temperature in degrees centigrade. (b) Variation of q_{cr} (Equation 3) for different salt concentrations since the onset of crystallization process (t_c). Positive and negative values of q_{cr} represent crystallization and dissolution, respectively. (c) An example of the details of heat fluxes associated with formation and dissolution of salt crystals and corresponding changes in surface temperature. The values of evaporative flux were extracted from mass loss measurements (Figure 2a). For the sake of modeling, the value of k_a was assumed to be constant at 0.0257 W/mK, while k_{soil} for saturated sand samples was measured using a thermal analyser (Meter, THEMPOS TR-3) as 2.3 W/mK. Recording of the thermal camera required for estimating mean surface temperature was disrupted for 1 day between days 10 and 12 for samples containing 20% NaCl.

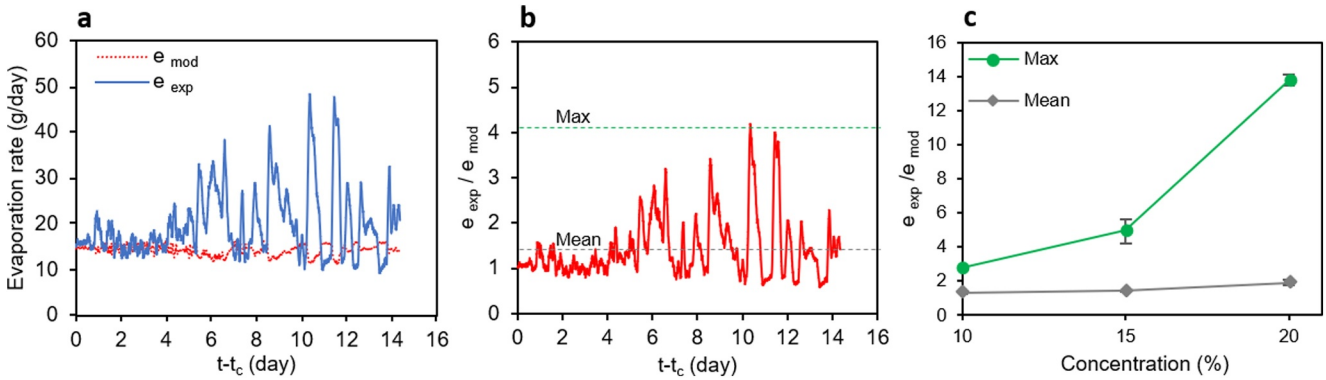

Figure 4. (a) Measured versus modeled evaporation rate from a sample of 15% NaCl (t_c in the horizontal axis stands for the onset of crystallization). (b) The ratio of the measured to the modeled evaporation rate (from an identical flat surface) indicates the role of the increased surface area with crystallization on evaporation dynamics. (c) The maximum, and mean ratio of the measured to the modeled evaporation rate for samples with different salt concentrations.

temperature associated with the formation and dissolution of crystals have also been observed by Shokri-Kuehni, Norouzi Rad, et al. (2017).

In this first-order analysis of surface fluxes, we have tacitly assumed a uniform flux of crystallization over the evaporating surface. However, the crystallization process at the threshold of nucleation occurs in clusters of salt crystals that may be very large relative to the time step. This rapid process stands in contrast to the linear dependency of evaporation rate on input energy and diffusion from the porous surface that are typically monotonous for fixed boundary conditions. Consequently, significant amounts of heat that are released over relatively short periods cause temperature spikes. These spikes provide the necessary energy for local enhancements of evaporative fluxes compared to the background evaporation cooling.

The coupling of evaporation rate and surface temperature at different salt concentrations will be further discussed in Section 3.4.

3.3. Effect of Crystallization on Evaporating Surface Area

The increase in surface roughness with formation of salt crystals (observed in optical images), may contribute in variation of evaporative losses from the salt samples. We can invoke Fick's law to quantify a diffusive water vapor flux (Gupta et al., 2014) and estimate the evaporation rate that would occur from an equivalent flat surface for a sample with an identical concentration of NaCl:

$$e = 86.4 \times 10^9 \frac{DA_f M}{\rho R T_s} \times \frac{P_s - P_a}{\delta} \quad (4)$$

in which e is the evaporation rate (g/day), A_f is the cross-sectional area of the sand columns (m^2), D is the water vapor diffusion coefficient in the air (m^2/s), ρ is the density of water (kg/m^3), M is the molecular mass of water (kg/mol), R is gas constant (J/mol K) and T_s is surface temperature (K). P_s and P_a are saturated vapor pressure at evaporating surface and vapor pressure in the air, respectively (Pa) (Shokri-Kuehni, Norouzi Rad, et al., 2017). The temperature data obtained from the IR camera was spatially averaged to represent the mean temperature of the evaporating surface.

The difference between the evaporation rates obtained from the balance and estimated based on Fick's law (Figure 4) shows the potential role of increased evaporating surface area on evaporation due to salt crystallization (see Figure S2 in Supporting Information S1). The ratio of the two evaporation rates is depicted in Figure 4b, which illustrates how the presence of salt crystals effectively increases the evaporating surface area, thereby enhancing evaporative losses from the samples (Licsandru & Prat, 2022). The maximum and mean ratios of increased surface area were plotted for samples saturated with 10%, 15%, and 20% NaCl in Figure 4c. Despite the impact of salinity reducing saturated vapor pressure, the data indicate that the increase in evaporating surface area as a result of salt crystallization, under the conditions implemented in our experiments, may result in an increase in evaporation rate by a factor of 3 to 14 (depending on the salt concentration).

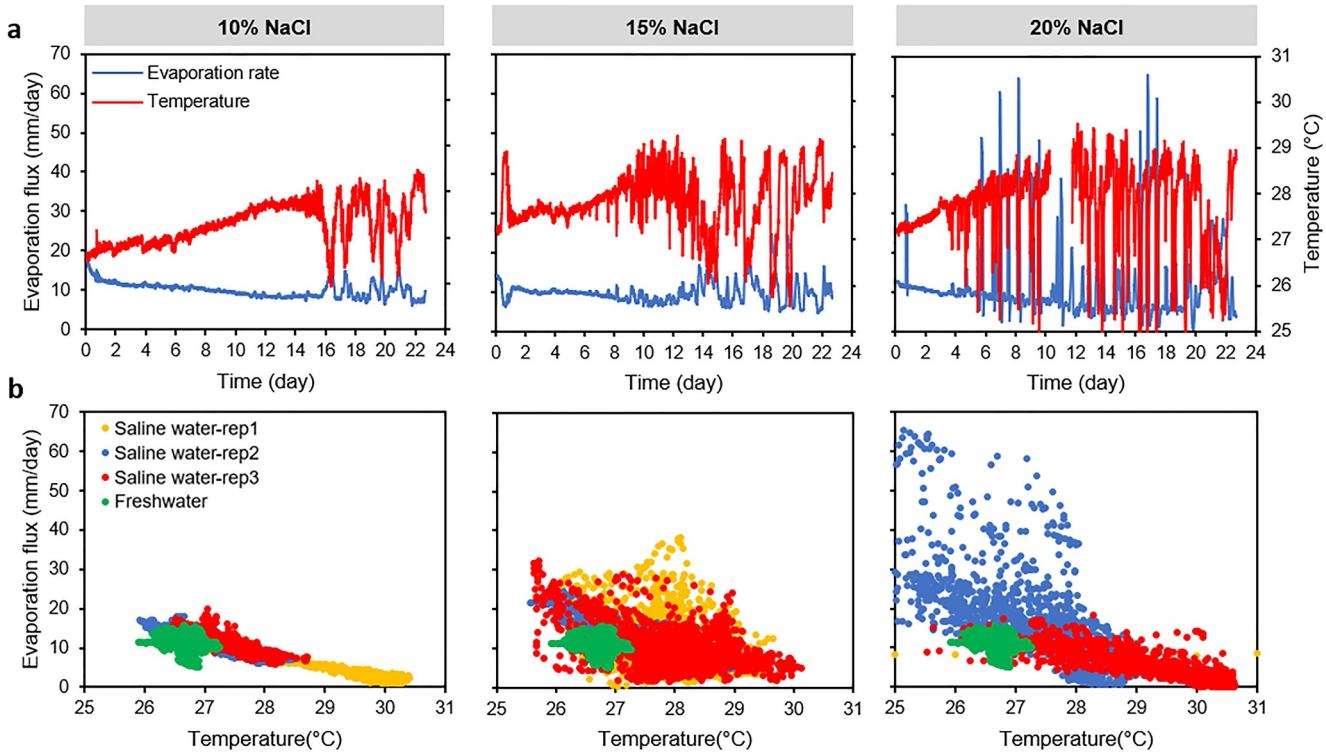

Figure 5. (a) Variations of evaporation flux and mean surface temperature over time for samples of 10%, 15%, and 20% NaCl solutions. The vertical axes on the left and right hand sides represent evaporation flux and surface temperature, respectively. The recording of the thermal camera was disrupted for 1 day between days 10 and 12 for samples containing 20% NaCl. (b) Evaporation flux versus mean surface temperature for samples with different NaCl concentrations.

3.4. The Coupling Between Surface Temperature and Evaporation Dynamics

We plotted variations of evaporation flux and associated changes in mean surface temperature of samples with different salt concentrations to investigate the impact of crystallization on the inherent coupling between heat and mass transfer processes over evaporating surfaces (Figure 5). The results show that fluctuations in evaporation flux are accompanied by variations in mean surface temperature of the samples. These findings demonstrate that the intermittent nature of evaporation dynamics from evaporating surfaces in the presence of salt crystals can further be inferred from thermal signatures of the surface. We also investigated the correlation between evaporation flux and surface temperature. As seen, the variation of evaporation flux is well-correlated with mean surface temperature at low salt concentrations (10%). However, the increase in salt concentration yielded a scattered relationship between evaporation and surface temperature. When crystallization is negligible (i.e., $q_{cr} \approx 0$), a linear correlation between evaporation flux (q_{evap}) and surface temperature (T_s) can be inferred from Equation 3 with linearization of longwave radiation flux (Aminzadeh & Or, 2014). Nevertheless, the flux of crystallization (q_{cr}) disrupts the linear correlation between evaporation flux and surface temperature as seen in samples with higher salt concentrations.

Such nuanced relationships between evaporation flux and surface temperature highlight the complexities that are involved in extracting dynamics of mass loss rates from saline surfaces using remotely sensed surface temperature signals at larger scales of interest (Holmes, 2019). The interplay between salt crystallization, temperature distribution, and evaporation rates suggests that accurate interpretation of remote sensing data for large-scale investigation of surface fluxes requires careful consideration of these intricate factors. The variability in surface temperature patterns due to salt presence complicates the direct correlation between surface temperature and evaporation fluxes, necessitating new models that account for the detailed thermodynamic and physical processes at play.

4. Conclusions

Evaporation experiments under controlled laboratory conditions were conducted to quantify the effect of salt crystals on evaporation from porous media. The results indicate that the presence of salt crystals may yield unpredictable evaporative patterns, even in samples with identical salt concentrations. We observed fluctuating evaporative mass loss rates, with the magnitude of these fluctuations increasing as salt concentration increased.

Moreover, analysis of thermal and optical images revealed the highly dynamic nature of crystallization, characterized by the nucleation and dissolution of salt crystals. These processes induce fluctuations in surface temperature indicating active contributions to water evaporation dynamics. Furthermore, the experiments suggest that the increased surface area resulting from crystallization could significantly enhance the evaporation rate.

Considerable heat fluxes associated with the crystallization process (as shown in Figure 3) could drastically influence the energy closure over evaporating terrestrial surfaces covered with salt crusts. This, in turn, affects the estimation of surface fluxes in present hydrological and climatological models. Such aspects are not considered in the present models for estimation of surface fluxes which require further research and investigation.

Data Availability Statement

The laboratory experimental data of this study was archived via Zenodo (Jannesarahmadi, 2024).

Acknowledgments
We gratefully acknowledge the financial support from the German Research Foundation (DFG), Grant 497539130, and the partial funding from DFG SFB 1313, project number 327154368. Resources provided by the Institute of Geo-Hydroinformatics at Hamburg University of Technology and technical assistance of Theodor Wassiliou in conducting laboratory experiments are greatly acknowledged. Open Access funding enabled and organized by Projekt DEAL.

References

Aminzadeh, M., Breitenstein, D., & Or, D. (2017). Characteristics of turbulent airflow deduced from rapid surface thermal fluctuations: An infrared surface anemometer. *Boundary-Layer Meteorology*, *165*(3), 519–534. https://doi.org/10.1007/s10546-017-0279-5

Aminzadeh, M., & Or, D. (2013). Temperature dynamics during nonisothermal evaporation from drying porous surfaces. *Water Resources Research*, *49*(11), 7339–7349. https://doi.org/10.1002/2013WR014384

Aminzadeh, M., & Or, D. (2014). Energy partitioning dynamics of drying terrestrial surfaces. *Journal of Hydrology*, *519*, 1257–1270. https://doi.org/10.1016/j.jhydrol.2014.08.037

Aminzadeh, M., Roderick, M. L., & Or, D. (2016). A generalized complementary relationship between actual and potential evaporation defined by a reference surface temperature. *Water Resources Research*, *52*(1), 385–406. https://doi.org/10.1002/2015WR017969

Bringedal, C., Schollenberger, T., Pieters, G. J. M., van Duijn, C. J., & Helmig, R. (2022). Evaporation-driven density instabilities in saturated porous media. *Transport in Porous Media*, *143*(2), 297–341. https://doi.org/10.1007/s11242-022-01772-w

Dashtian, H., Shokri, N., & Sahimi, M. (2018). Pore-network model of evaporation-induced salt precipitation in porous media: The effect of correlations and heterogeneity. *Advances in Water Resources*, *112*(2017), 59–71. https://doi.org/10.1016/j.advwatres.2017.12.004

Dashtian, H., Wang, H., & Sahimi, M. (2017). Nucleation of salt crystals in clay minerals: Molecular dynamics simulation. *Journal of Physical Chemistry Letters*, *8*(14), 3166–3172. https://doi.org/10.1021/acs.jpclett.7b01306

Derluyn, H. (2012). *Salt transport and crystallization in porous limestone: Neutron-X-ray imaging and poromechanical modeling* Doctoral dissertation. ETH Zurich.

Derluyn, H., Moonen, P., & Carmeliet, J. (2014). Deformation and damage due to drying-induced salt crystallization in porous limestone. *Journal of the Mechanics and Physics of Solids*, *63*(1), 242–255. https://doi.org/10.1016/j.jmps.2013.09.005

Eloukabi, H., Sghaier, N., Ben Nasrallah, S., & Prat, M. (2013). Experimental study of the effect of sodium chloride on drying of porous media: The crusty–patchy efflorescence transition. *International Journal of Heat and Mass Transfer*, *56*(1–2), 80–93. https://doi.org/10.1016/j.ijheatmasstransfer.2012.09.045

Espinosa-Marzal, R. M., & Scherer, G. W. (2010). Mechanisms of damage by salt. *Geological Society - Special Publications*, *331*(2012), 61–77. https://doi.org/10.1144/SP331.5

Gupta, S., Huinink, H. P., Pel, L., & Kopinga, K. (2014). How ferrocyanide influences NaCl crystallization under different humidity conditions. *Crystal Growth & Design*, *14*(4), 1591–1599. https://doi.org/10.1021/cg4015459

Hassani, A., Azapagic, A., D'Odorico, P., Keshmiri, A., & Shokri, N. (2020). Desiccation crisis of saline lakes: A new decision-support framework for building resilience to climate change. *Science of the Total Environment*, *703*, 134718. https://doi.org/10.1016/j.scitotenv.2019.134718

Hassani, A., Smith, P., & Shokri, N. (2024). Negative correlation between soil salinity and soil organic carbon variability. *Proceedings of the National Academy of Sciences of the United States of America*, *121*(18). https://doi.org/10.1073/pnas.2317332121

Holmes, T. R. H. (2019). Remote sensing techniques for estimating evaporation. In *Extreme hydroclimatic events and multivariate hazards in a changing environment* (pp. 129–143). Elsevier. https://doi.org/10.1016/B978-0-12-814899-0.00005-5

Jambhekar, V. A., Mejri, E., Schröder, N., Helmig, R., & Shokri, N. (2016). Kinetic approach to model reactive transport and mixed salt precipitation in a coupled free-flow–porous-media system. *Transport in Porous Media*, *114*(2), 341–369. https://doi.org/10.1007/s11242-016-0665-3

Jannesarahmadi, S. (2024). Quantifying salt crystallization impact on evaporation dynamics from porous surfaces [Dataset]. *Zenodo*. https://doi.org/10.5281/zenodo.12545536

Jannesarahmadi, S., Aminzadeh, M., Raga, R., & Shokri, N. (2023). Effects of microplastics on evaporation dynamics in porous media. *Chemosphere*, *311*(P1), 137023. https://doi.org/10.1016/j.chemosphere.2022.137023

Lasser, J., Ernst, M., & Goehring, L. (2021). Stability and dynamics of convection in dry salt lakes. *Journal of Fluid Mechanics*, *917*, A14. https://doi.org/10.1017/jfm.2021.225

Lasser, J., Nield, J. M., Ernst, M., Karius, V., Wiggs, G. F. S., Threadgold, M. R., et al. (2023). Salt polygons and porous media convection. *Physical Review X*, *13*(1), 011025. https://doi.org/10.1103/PhysRevX.13.011025

Lazhar, R., Najjari, M., & Prat, M. (2020). Combined wicking and evaporation of NaCl solution with efflorescence formation: The efflorescence exclusion zone. *Physics of Fluids*, *32*(6). https://doi.org/10.1063/5.0007548

Lepinay, S. E. G., Nijveld, R., Velikov, K. P., & Shahidzadeh, N. (2022). NaCl crystals as carriers for micronutrient delivery. *ACS Omega*, *7*(33), 28955–28961. https://doi.org/10.1021/acsomega.2c02572

Licsandru, G., Noiriel, C., Duru, P., Geoffroy, S., Abou-Chakra, A., & Prat, M. (2023). Evaporative destabilization of a salt crust with branched pattern formation. *Scientific Reports*, *13*(1), 1–15. https://doi.org/10.1038/s41598-023-31640-6

Licsandru, G., Noiriel, C., Geoffroy, S., Abou-Chakra, A., Duru, P., & Prat, M. (2022). Detachment mechanism and reduced evaporation of an evaporative NaCl salt crust. *Scientific Reports*, *12*(1), 7473. https://doi.org/10.1038/s41598-022-11541-w

Licsandru, G., & Prat, M. (2022). Enhanced transport in a porous medium due to dissolved salt. *Physical Review Fluids*, *7*(6), 064304. https://doi.org/10.1103/PhysRevFluids.7.064304

Misyura, S. Y. (2018). Evaporation and heat transfer of aqueous salt solutions during crystallization. *Applied Thermal Engineering*, *139*, 203–212. https://doi.org/10.1016/j.applthermaleng.2018.04.068

Misyura, S. Y. (2020). The crystallization behavior of the aqueous solution of $CaCl_2$ salt in a drop and a layer. *Scientific Reports*, *10*(1), 256. https://doi.org/10.1038/s41598-019-57169-1

Misyura, S. Y. (2021). Different modes of heat transfer and crystallization in a drop of NaCl solution: The influence of key factors on the crystallization rate and the heat transfer coefficient. *International Journal of Thermal Sciences*, *159*, 106602. https://doi.org/10.1016/j.ijthermalsci.2020.106602

Nachshon, U., Shahraeeni, E., Or, D., Dragila, M., & Weisbrod, N. (2011). Infrared thermography of evaporative fluxes and dynamics of salt deposition on heterogeneous porous surfaces. *Water Resources Research*, *47*(12), 1–16. https://doi.org/10.1029/2011WR010776

Nachshon, U., & Weisbrod, N. (2015). Beyond the salt crust: On combined evaporation and subflorescent salt precipitation in porous media. *Transport in Porous Media*, *110*(2), 295–310. https://doi.org/10.1007/s11242-015-0514-9

Nachshon, U., Weisbrod, N., Dragila, M. I., & Grader, A. (2011). Combined evaporation and salt precipitation in homogeneous and heterogeneous porous media. *Water Resources Research*, *47*(3), 1–16. https://doi.org/10.1029/2010WR009677

Nachshon, U., Weisbrod, N., Katzir, R., & Nasser, A. (2018). NaCl crust architecture and its impact on evaporation: Three-dimensional insights. *Geophysical Research Letters*, *45*(12), 6100–6108. https://doi.org/10.1029/2018GL078363

Nield, D. A., & Bejan, A. (2017). *Convection in porous media* (5th ed.). Springer.

Nield, J. M., Bryant, R. G., Wiggs, G. F. S., King, J., Thomas, D. S. G., Eckardt, F. D., & Washington, R. (2015). The dynamism of salt crust patterns on playas. *Geology*, *43*(1), 31–34. https://doi.org/10.1130/G36175.1

Norouzi Rad, M., Shokri, N., Keshmiri, A., & Withers, P. J. (2015). Effects of grain and pore size on salt precipitation during evaporation from porous media. *Transport in Porous Media*, *110*(2), 281–294. https://doi.org/10.1007/s11242-015-0515-8

Norouzi Rad, M., Shokri, N., & Sahimi, M. (2013). Pore-scale dynamics of salt precipitation in drying porous media. *Physical Review*, *88*(3), 032404. https://doi.org/10.1103/PhysRevE.88.032404

Rodriguez-Navarro, C., & Doehne, E. (1999). Salt weathering: Influence of evaporation rate, supersaturation and crystallization pattern. *Earth Surface Processes and Landforms*, *24*(3), 191–209. https://doi.org/10.1002/(SICI)1096-9837(199903)24:3<191::AID-ESP942>3.0.CO;2-G

Sghaier, N., Geoffroy, S., Prat, M., Eloukabi, H., & Ben Nasrallah, S. (2014). Evaporation-driven growth of large crystallized salt structures in a porous medium. *Physical Review*, *90*(4), 042402. https://doi.org/10.1103/PhysRevE.90.042402

Sghaier, N., & Prat, M. (2009). Effect of efflorescence formation on drying kinetics of porous media. *Transport in Porous Media*, *80*(3), 441–454. https://doi.org/10.1007/s11242-009-9373-6

Shahidzadeh-Bonn, N., Rafaï, S., Bonn, D., & Wegdam, G. (2008). Salt crystallization during evaporation: Impact of interfacial properties. *Langmuir*, *24*(16), 8599–8605. https://doi.org/10.1021/la8005629

Shahraeeni, E., & Or, D. (2010). Thermo-evaporative fluxes from heterogeneous porous surfaces resolved by infrared thermography. *Water Resources Research*, *46*(9). https://doi.org/10.1029/2009WR008455

Shokri-Kuehni, S. M. S., Bergstad, M., Sahimi, M., Webb, C., & Shokri, N. (2018). Iodine k-edge dual energy imaging reveals the influence of particle size distribution on solute transport in drying porous media. *Scientific Reports*, *8*(1), 1–9. https://doi.org/10.1038/s41598-018-29115-0

Shokri-Kuehni, S. M. S., Norouzi Rad, M., Webb, C., & Shokri, N. (2017). Impact of type of salt and ambient conditions on saline water evaporation from porous media. *Advances in Water Resources*, *105*, 154–161. https://doi.org/10.1016/j.advwatres.2017.05.004

Shokri-Kuehni, S. M. S., Raaijmakers, B., Kurz, T., Or, D., Helmig, R., & Shokri, N. (2020). Water table depth and soil salinization: From pore-scale processes to field-scale responses. *Water Resources Research*, *56*(2). https://doi.org/10.1029/2019WR026707

Shokri-Kuehni, S. M. S., Sahimi, M., & Shokri, N. (2022). A personal perspective on prediction of saline water evaporation from porous media. *Drying Technology*, *40*(4), 691–696. https://doi.org/10.1080/07373937.2021.1999256

Shokri-Kuehni, S. M. S., Vetter, T., Webb, C., & Shokri, N. (2017). New insights into saline water evaporation from porous media: Complex interaction between evaporation rates, precipitation, and surface temperature. *Geophysical Research Letters*, *44*(11), 5504–5510. https://doi.org/10.1002/2017GL073337

Wooding, R. A., Tyler, S. W., & White, I. (1997). Convection in groundwater below an evaporating Salt Lake: 1. Onset of instability. *Water Resources Research*, *33*(6), 1199–1217. https://doi.org/10.1029/96WR03533